MAX-PLANCK-INSTITUT FÜR PLASMAPHYSIK

GARCHING BEI MÜNCHEN

NEUTRAL BEAM INJECTION CALCULATIONS FOR TORSATRONS

D.T. Anderson and J.L. Shohet[+)]
S. Rehker
J.A. Tataronis[++)]

IPP 6/189 October 1979

[+)] University of Wisconsin, Madison, WI. 53706 (USA)

[++)] Courant Institute, New York University, New York, N.Y. 10012 (USA)

Die nachstehende Arbeit wurde im Rahmen des Vertrages zwischen dem Max-Planck-Institut für Plasmaphysik und der Europäischen Atomgemeinschaft über die Zusammenarbeit auf dem Gebiete der Plasmaphysik durchgeführt.

ABSTRACT

A numerical investigation of the effectiveness of neutral beam heating in two torsatron-type devices has been undertaken. A modified version of a well known deposition and orbit code was used for this purpose. It was found that, for beam currents within the applicable range of the model, neutral beams can efficiently heat either a "classical" torsatron or an "ultimate" torsatron plasma provided the injection is tangential to the magnetic axis. These results were obtained by following ionized test particles down to thermalization. Efficiency of the injection drops as the angle approaches perpendicular due to relatively poor containment of helically trapped orbits within the volume specified by a fixed cutoff radius.

I. INTRODUCTION

Neutral beam injection is the next large step that must be taken in the heating of torsatron/stellarator type devices, especially in the light of drift parameter scaling previously reported in the Cleo stellarator, [1] and now reported in the L-2 stellarator[2]. Modest neutral injection has been employed on the Cleo and W-VIIa stellarators with encouraging results, but the available injected power is limited due to the relatively small spacing between the helical windings. It appears that high power neutral injection must wait until larger machines are available. Looking forward to this time, injection has been examined numerically in both a classical torsatron[3] and an ultimate torsatron[4] of large dimensions. A torsatron configuration has been chosen for its relatively large access. The purpose of this paper is to show that neutral beam injection can efficiently heat either a classical or an ultimate torsatron, and is not a comparison of the relative merits of the two different devices.

The physical parameters of two torsatrons are summarized in Table I.

Device	Winding Law	ℓ	Field Periods	R(m)	r(m)	B_T(kG)
Classical	$\phi=m\theta$	3	16	3.06	.50	30
Ultimate	$\phi=m\theta+\alpha\sin\phi$ $\alpha=.63$	2	12	2.50	.56	30

Table I

As evidenced in Table I, the machines have different poloidal and toroidal multiplicities as well as different major and minor radii, obviating any direct comparison.

Similar plasma parameters were assumed for each device. Both temperature and density profiles were assumed to be of the double parabolic type, with a minimum electron temperature of 100 eV. The neutral gas profile (due to base vacuum) was assumed to be of the form:

$$n_0(r) = 2 \times 10^8 + 1.8 \times 10^9 \times e^{\left(\frac{r-r_{wall}}{4.}\right)} \text{ particles/cm}^3$$

corresponding to a base pressure which varies from 7×10^{-9} Torr to 7×10^{-8} Torr. r is in centimeters.

Injection into plasmas with peak electron temperatures of 500 eV and peak densities of 1×10^{14} (particles/cm^3) was examined. These parameters were chosen as reasonable values for a target plasma formed from an ohmic heating pulse.

II. DESCRIPTION OF THE NUMERICAL CODE

The neutral beam heating calculations were computed using a modified[5] version of the Dei-Cas tokamak neutral injection code[6]. This code is fully three dimensional in both fields and particle orbits. The fields are calculated using a Biot-Savart formulation, and are not derived from expansions. All relevant profiles are single dimensional in the minor radial coordinate. The injection is modeled using single particle guiding center orbits, with a reduction in energy corresponding to the Spitzer electron drag slowing down time[7]

$$\tau_s = A_f \frac{T_e^{3/2} 6.27 \times 10^8}{N_e \ln \Lambda} \quad (s, eV, cm^{-3})$$

Features of the code include:

1) Neutral particles are ionized along a filamentary injection line by proton impact, electron impact, and charge-exchange, dependent upon plasma profiles.
2) Each fast ion born is assigned a weight corresponding to the fraction of the beam which would be ionized at that location, i.e. $\sum_i (\text{weight})_i + (\text{not ionized}) = 1$.
3) Up to fifty particles may be used to model each injection sequence. The calculations presented here used twenty particles per run to reduce CPU time required.
4) Each fast ion born is assigned another initial weight of 1.0 which is reduced during the thermalization by effects of charge-exchange.
5) Once this charge-exchange weight is reduced, no re-exchange is allowed, making the code conservative in this respect.
6) Orbits are followed using a single-particle guiding center model with an Adams integrator. The energy of the fast ion is reduced during the orbit calculation by using a slowing down time argument to model the transfer of energy from the fast ions to the bulk plasma.
7) Orbits which extend beyond a determined minor radius are "cut-off", in effect putting in a limiter or wall.
8) To calculate the confinement probability of the fast ions we follow the trajectories during the slowing down, taking into account the actual local magnetic field (zero beta) and the plasma parameters with their associated profiles. Pitch angle scattering is modeled by a random walk process of the Monte-Carlo type.

The Dei-Cas code uses a filamentary injection line, and hence, any effects of beam optics are not included. The beam is also assumed to be mono-energetic, so the one-half as well as other energy components are not accounted for in a single run.

For the devices examined, along with the assumed plasma profiles, a variation of the beam energy yielded an optimum injection energy of around forty kilovolts. Particles which have energies much lower than this ($\sim$ 20 keV) give birth to fast ions at large minor radii and penetration into the plasma is low. Particles of higher energies ($\sim$ 60 keV) gave good penetration, but there existed significant amounts of the beam which punched through to the inside wall of the device for large injection angles. For these reasons 40 keV was chosen as the injection energy for this study. As mentioned previously, with this modelling the beam current is not taken into account, and arbitrary power levels may be assumed as long as the slowing down time argument for the parameters assumed is still valid. Of course, when there is a significant amount of energy density in the beam as compared to the background plasma the formulation breaks down and awaits a full Fokker-Planck type treatment.

III. INJECTION EFFICIENCY VERSUS INJECTION ANGLE

Injection efficiency was studied in the two devices previously mentioned as a function of the angle of injection with respect to the magnetic axis. The neutral beam was composed of hydrogen on a target plasma also of hydrogen. z_{eff} was taken to be unity, since all recent stellarator results have pointed to relatively clean machine operation; most probably due to the confining field existing before plasma formation. The beam energy was taken to be forty

kilovolts. The target plasma profiles are exhibited in Figures 1-3, showing temperature, plasma density, and neutral gas density. These were taken to be the same in the classical and ultimate torsatron, with only a slight difference in scale length. Figures 4 and 5 show the ionization profiles for the ultimate and classical torsatrons respectively, for 3 separate injection angles. The slight difference between the two sets of ionization profiles is due solely to the difference in scale length since the same plasma and beam parameters are assumed for both cases. Superimposed upon the ionization plots in Figures 4 and 5 are the actual heating profiles (labelled thermalization) calculated by observing where the fast ions give up their energy. In most cases, the heating profiles can be seen to be quite distinct from the ionization profiles. Figure 6 shows a plot of both ionization and thermalization efficiencies versus angle for the two configurations. It is easily seen from Figure 6 that the thermalization efficiency is a much more sensitive function of angle than is the ionization. Note that the thermalization efficiency of the ultimate torsatron is less than the classical torsatron. The basic reason appears to be due to increased magnetic field ripple. This results from the lower aspect ratio and the fewer number of field periods in the particular ultimate torsatron configuration used in these calculations compared to the classical torsatron. As a result, a direct comparison is not meaningful. However, tangential injection appears to be equally efficient for both configurations.

While the ionization profiles depend only on the path length (with given profiles), the thermalization profiles are generated by the actual fast ion orbits, which depend upon magnetic configuration

and initial conditions of the fast ions, as well as the effects of charge-exchange and direct orbit losses related to the fast ion containment probability. As mentioned in the description of the code, fast ions whose orbits extend beyond a specified minor radius are presumed lost. In the computations presented here the cut-off was set to approximately half-way between the separatrix radius and the helical winding radius.

IV. ORBITS

Insight may be gained to the angular dependence of the injection by examining the different types of orbits in the various cases. Circulating particles are well-behaved, being confined by the flux surfaces. Good confinement of trapped particles is observed only for those fast trapped ions born well inside the separatrix. Trapped particles born near the separatrix have orbits with large radii and strike the cut-off boundary. This effect may be artificial in a device with no material wall inside the helical windings. In this sense, confinement of trapped particles is estimated pessimistically by the code since it is possible that their orbits could bring them back to the confinement zone. The loss of trapped particles whose orbits extend to the cut-off radius creates an effective hole in velocity space at large pitch angles.

The relative success of tangential injection can be viewed as a relationship between the time it takes the fast ion to scatter to the hole in velocity space at large pitch angles and the time it takes to slow down and deposit its energy in the bulk plasma.

For tangentially injected neutrals, the fast ions are born with low pitch angles and have a 90° scattering time (for the parameters selected) of 7-9 milliseconds, as compared to a slowing down time on the order of 5 milliseconds. Figure 7 is a plot of such an injected circulating particle. During the course of slowing down, a fast ion typically undergoes 1800-2200 small angle collisions denoted on the orbit plots as "+" signs. For clarity, the plots do not follow the particle all the way down to thermalization. In all of the tangential injection runs, no circulating fast ions were seen to scatter to a trapped state. Losses for tangential injection in these calculations were only due to charge-exchange and to birth of fast ions external to the separatrix. Due to the constant, Monte-Carlo, small angle, coulomb collisions which are occurring, the fast ions may change their orbit state during the course of slowing down.

As the angle of injection is moved towards the perpendicular, characteristics of the orbits change. Since the distance in pitch angle space to a trapped state is now reduced, fast ions, which were initially circulating can now scatter into trapped states. This is illustrated in Figure 8. As a result, only part of the fast ions' energy is given to the bulk plasma before it is lost. Direct orbit loss now begins to have an effect on efficiency. It should be pointed out, however, that fast ions initially of the circulating type, and then scattered to trapped states, can scatter back to a different circulating orbit. Also, not all trapped particles are lost, and thus position also affects the function of particles lost. Figure 9 is a plot of the orbit of a fast ion produced by perpendicular injection. While the orbit is not closed and wanders over the minor

cross-section, it is contained down to thermalization.

IV. CONCLUSIONS

These calculations point out the necessity of injecting neutrals in a torsatron in a fashion which will give them the largest parallel component of velocity possible. Since the primary direction of the field is toroidal, this can be accomplished by injecting in as toroidal a direction as possible, i.e. tangential to the magnetic axis.

V. ACKNOWLEDGEMENTS

This work was supported by the U.S. Department of Energy under contract No. ET-78-S-02-5069.

Figure Captions

1) Electron temperature profile

2) Electron density profile

3) Neutral gas density profile

4) Thermalization and ionization profiles for the ultimate torsatron configuration
   a) tangential injection- per cent not ionized $\sim 10^{-3}$, thermalization efficiency ~82%
   b) 55° off-tangential injection- percent not ionized ~ 7, thermalization efficiency ~ 49%
   c) perpendicular injection - per cent not ionized ~ 11, thermalization efficiency ~ 10%

5) Thermalization and ionization profiles for the classical torsatron configuration
   a) tangential injection - per cent not ionized ~ 10^{-3} thermalization efficiency ~ 82%
   b) 65° off-tangential injection - per cent not ionized ~ 8 thermalization efficiency ~ 52%
   c) perpendicular injection - per cent not ionized ~ 11 thermalization efficiency ~ 40%

6) Ionization and thermalization efficiencies as a function of injection angle."A" corresponds to the ultimate torsatron. "B" corresponds to the classical torsatron.

7) Guiding center trajectory of a circulating particle injected at 65°.

8) Guiding center trajectory of a circulating particle injected at an angle of 65° which scatters to a trapped state and is lost.

9) Guiding center trajectory of a trapped particle injected perpendicularly which is contained to thermalization.

References

1) D. W. Atkinson, D. Bartlett, J. Bradley, A. N. Dellis, S. M. Hamberger, D. J. Lees, J. B. Lister, W. Millar, L. E. Sharp, P. A. Shatford, in Proc. VIII European Conference on Controlled Fusion and Plasma Physics, Prague, 1977.

2) M. S. Rabinovich, Lebedev Institute Preprint #27, February 1979 (in Russian).

3) C. Gourdon, D. Marty, E. K. Maschke, J. O. Dumont, in Plasma Physics and Controlled Nuclear Fusion Research (Proc. 3rd Int. Conf., Novosibirsk, 1968) 1, IAEA, Vienna (1969).

4) C. Gourdon, P. Hubert, D. Marty, C. R. Acad. Sc. Paris, Vol. 271, (1970).

5) S. Rehker, Max Planck IPP Report 2/237 (1978).

6) R. Dei-Cas, private communication.

7) L. Spitzer, Jr., Physics of Fully Ionized Gases, 2nd ed. Wiley Interscience, New York (1962).

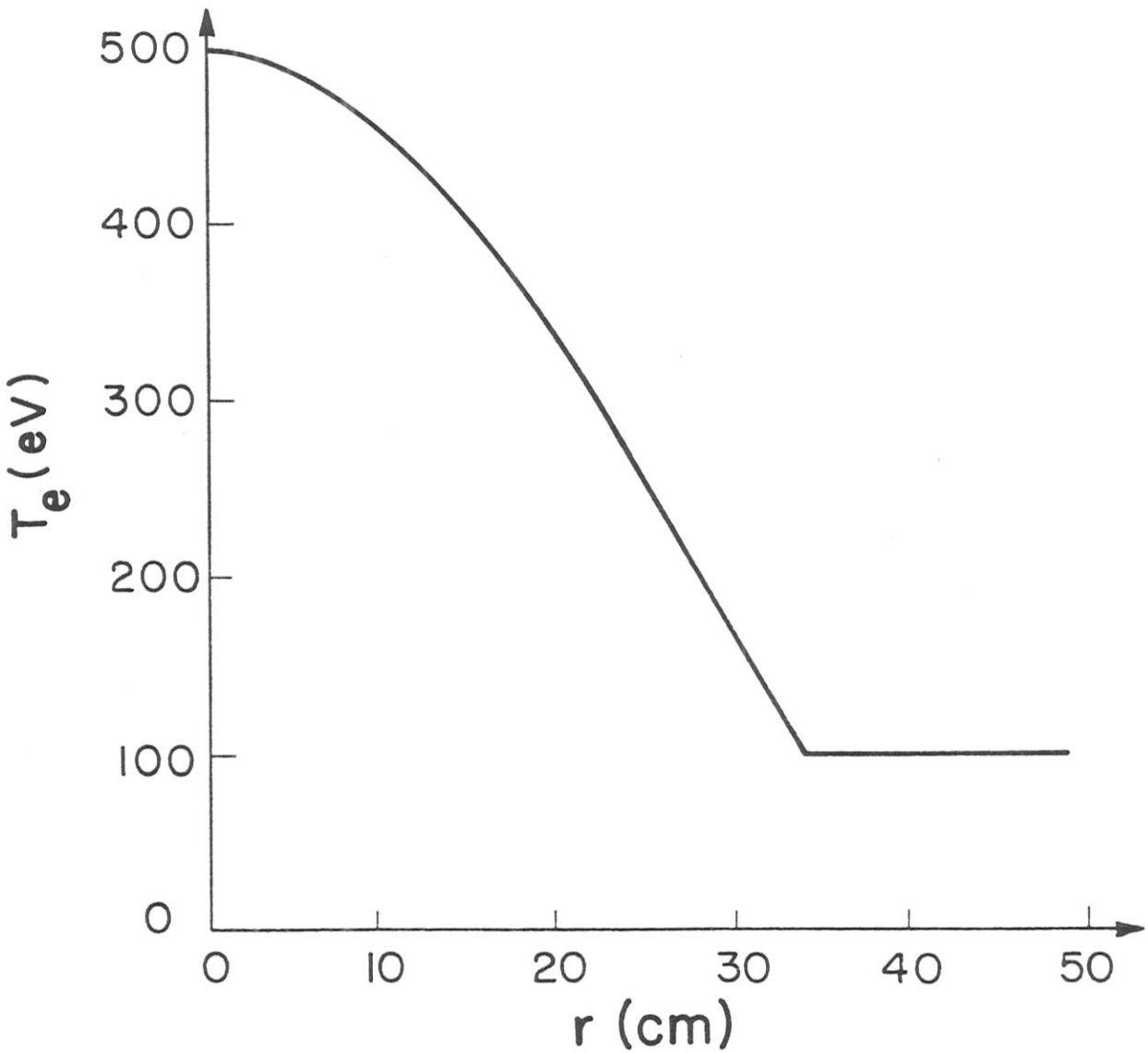

Figure 1

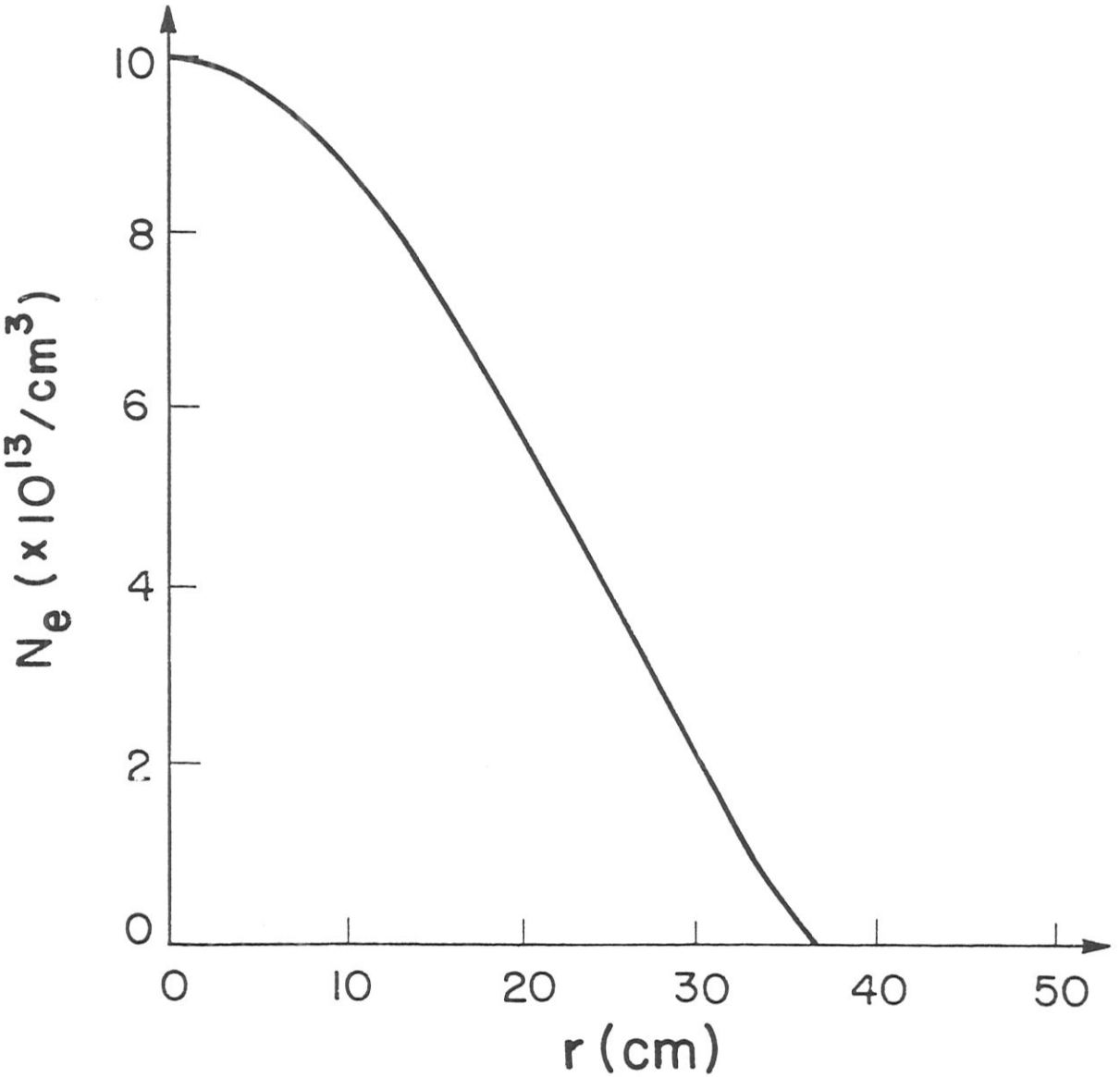

Figure 2

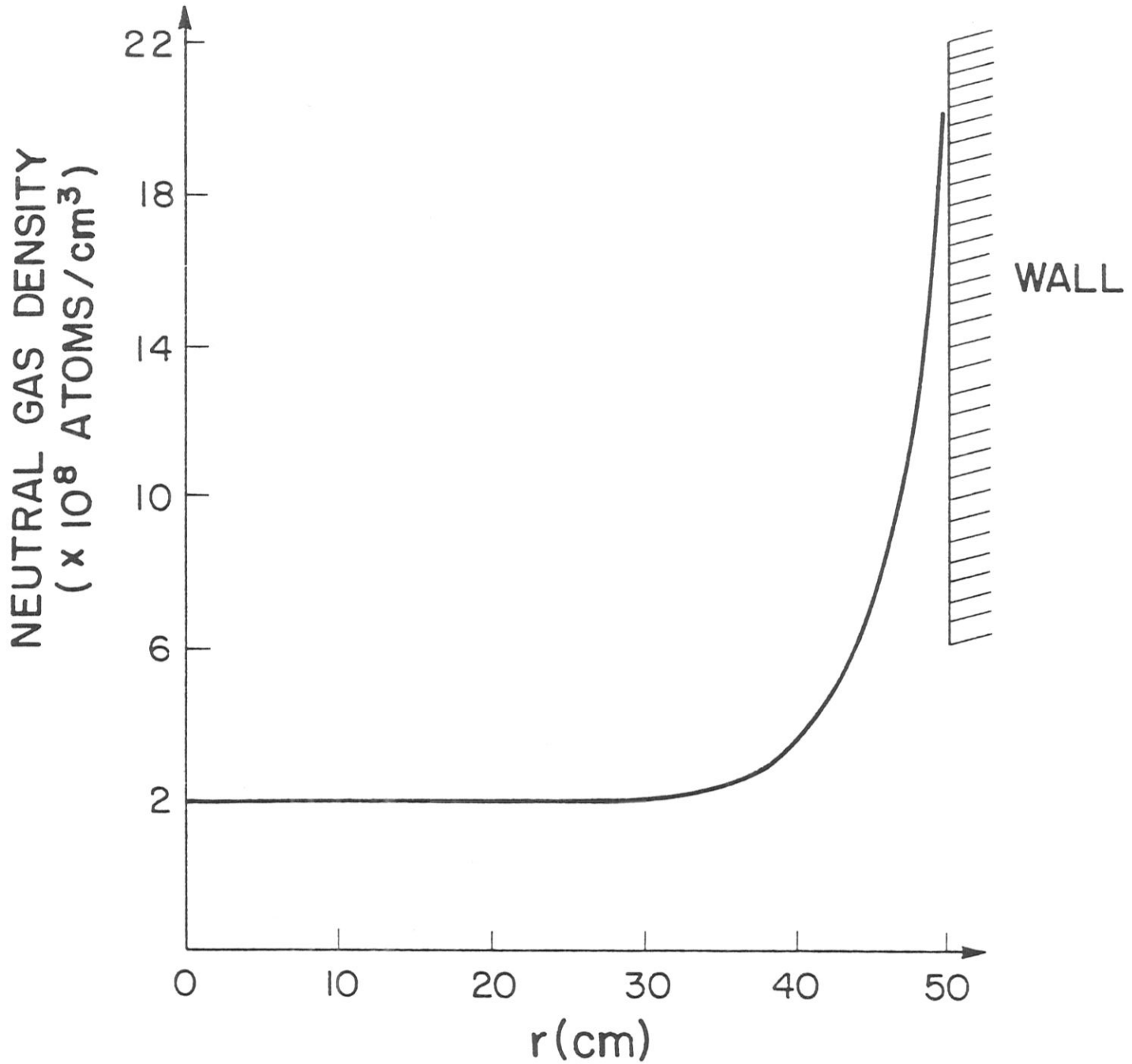
NEUTRAL GAS DENSITY
(x 10⁸ ATOMS/cm³)
22
18
14
10
6
2
0
10
20
30
40
50
r(cm)
WALL

Figure 3

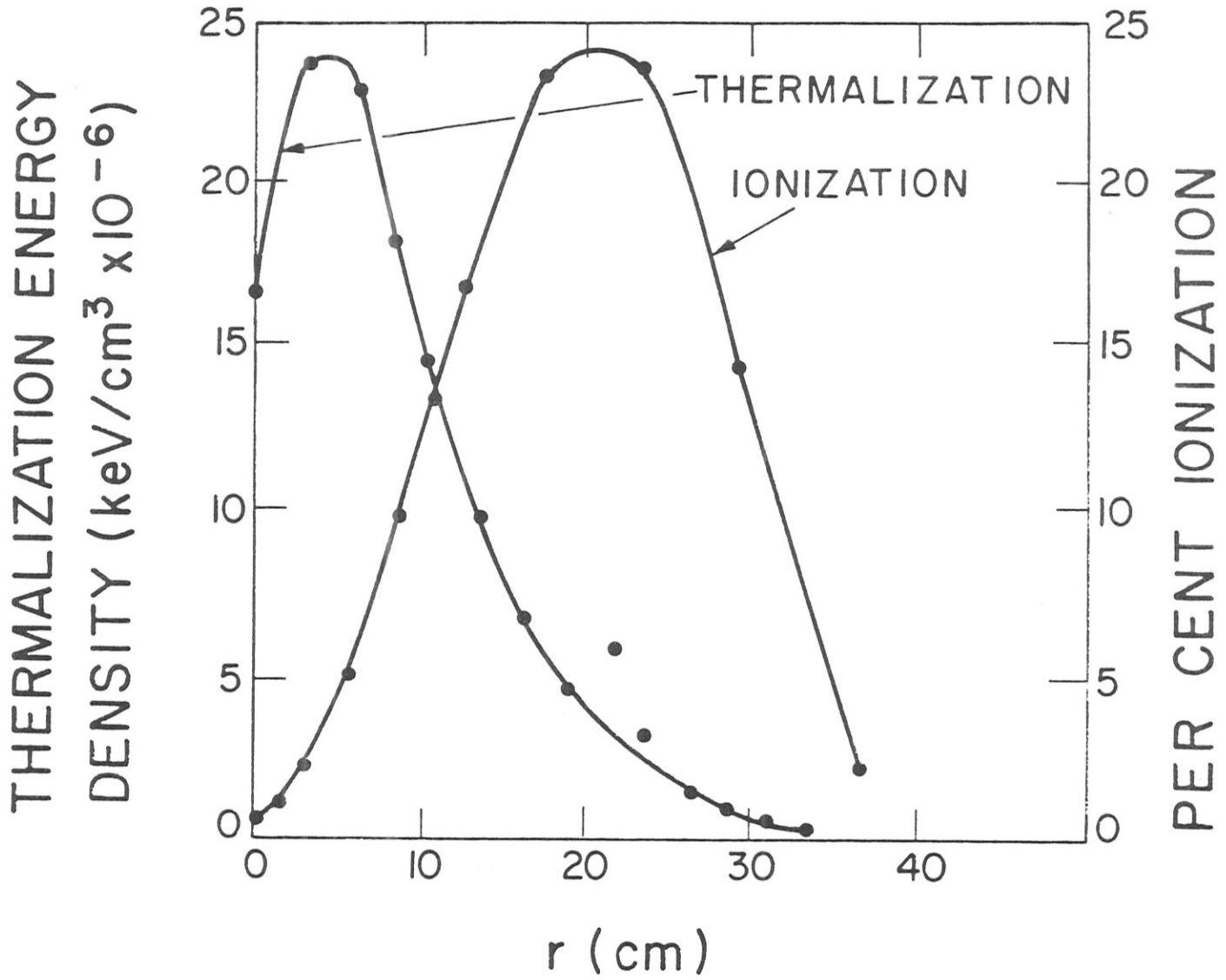
THERMALIZATION ENERGY DENSITY (keV/cm³ x10⁻⁶)
PER CENT IONIZATION
THERMALIZATION
IONIZATION
r (cm)
0
5
10
15
20
25
0
10
20
30
40

Figure 4 a

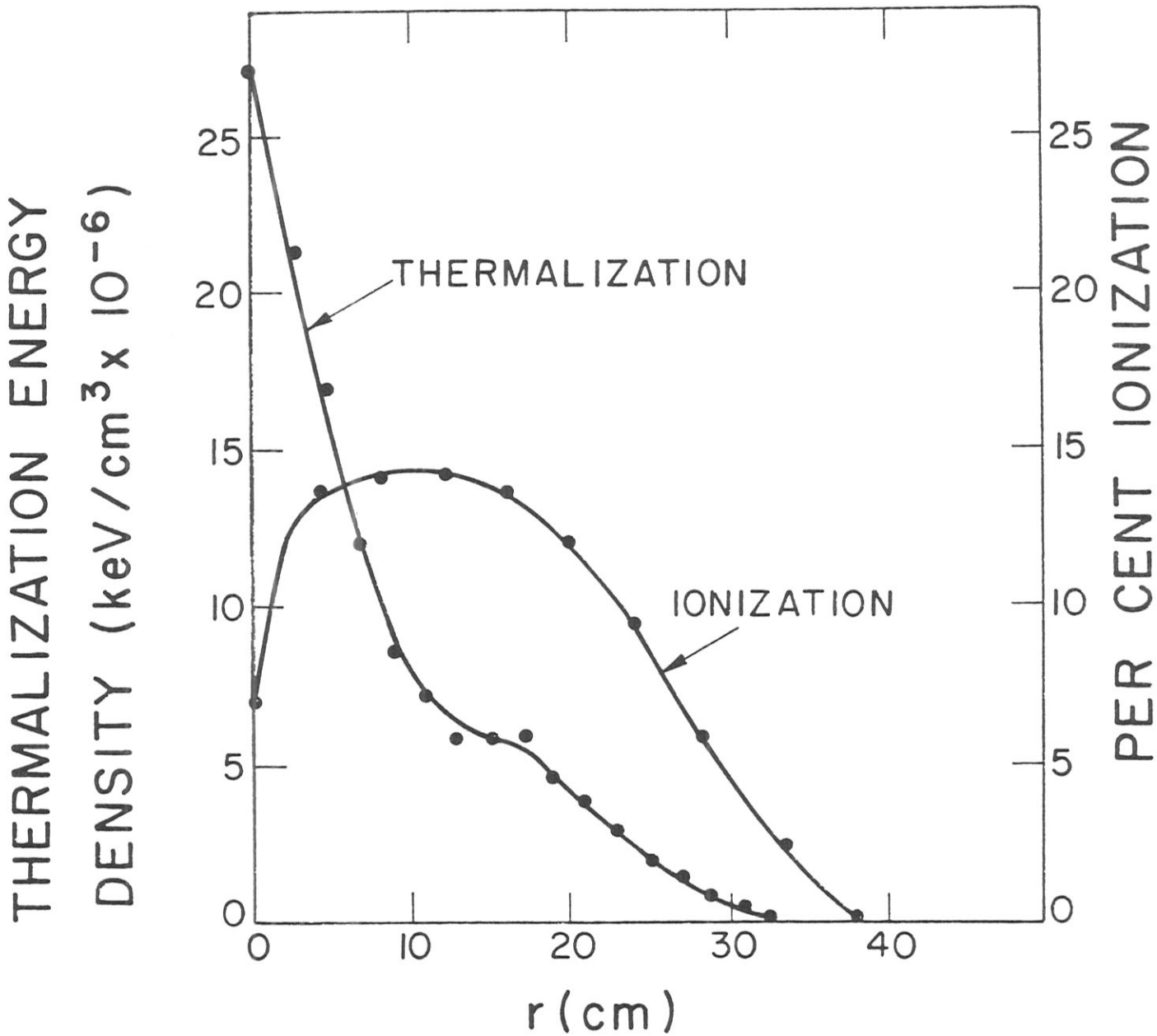
THERMALIZATION ENERGY DENSITY (keV/cm³ x 10⁻⁶)
PER CENT IONIZATION
THERMALIZATION
IONIZATION
r (cm)
0
5
10
15
20
25
0
10
20
30
40

Figure 4b

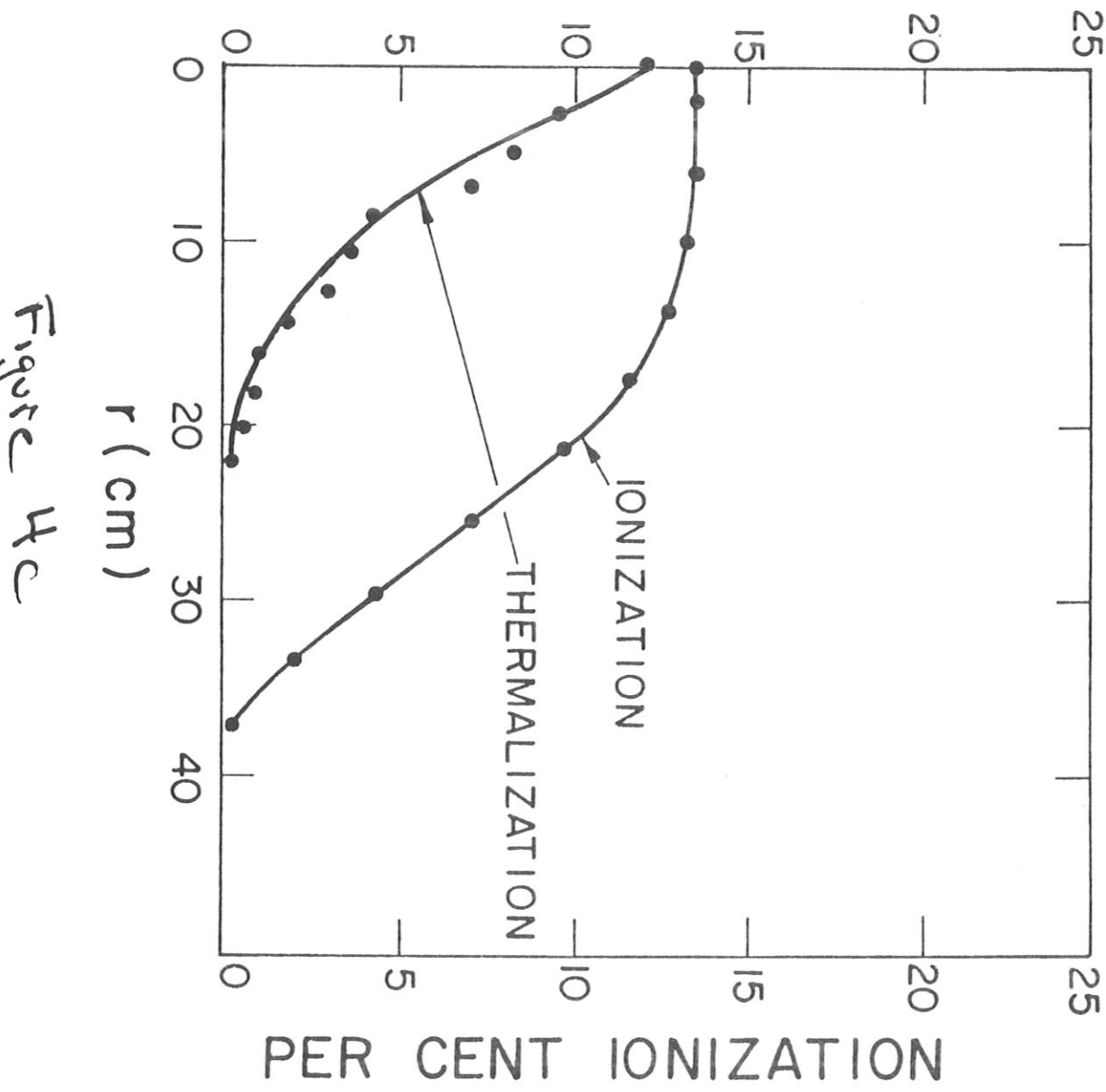
THERMALIZATION ENERGY
DENSITY (keV/cm³ x 10⁻⁶)
0
5
10
15
20
25
r (cm)
0
10
20
30
40
IONIZATION
THERMALIZATION
PER CENT IONIZATION

Figure 4c

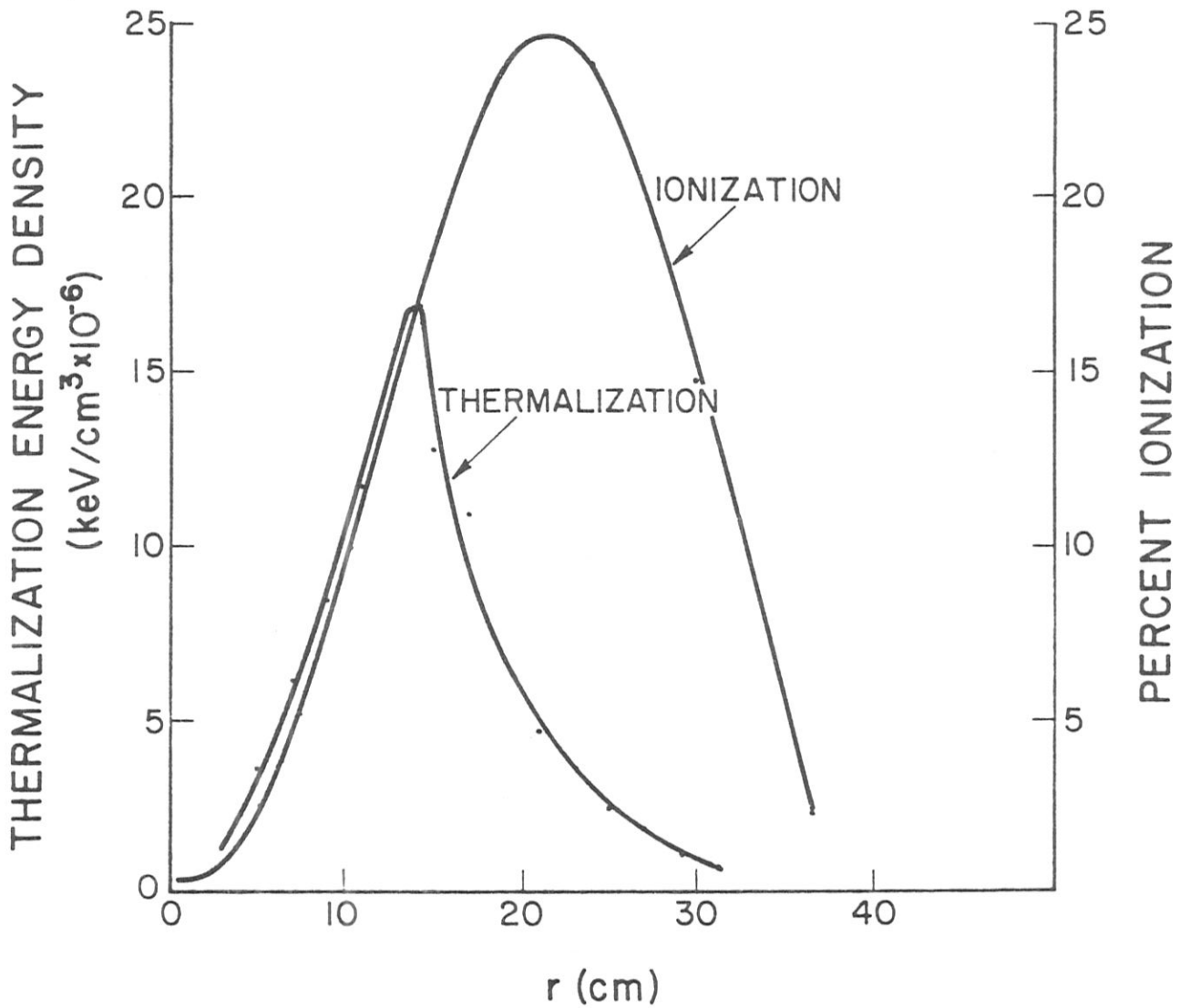
THERMALIZATION ENERGY DENSITY
(keV/cm³×10⁻⁶)
PERCENT IONIZATION
IONIZATION
THERMALIZATION
r (cm)
0
5
10
15
20
25
0
10
20
30
40

Figure 5a

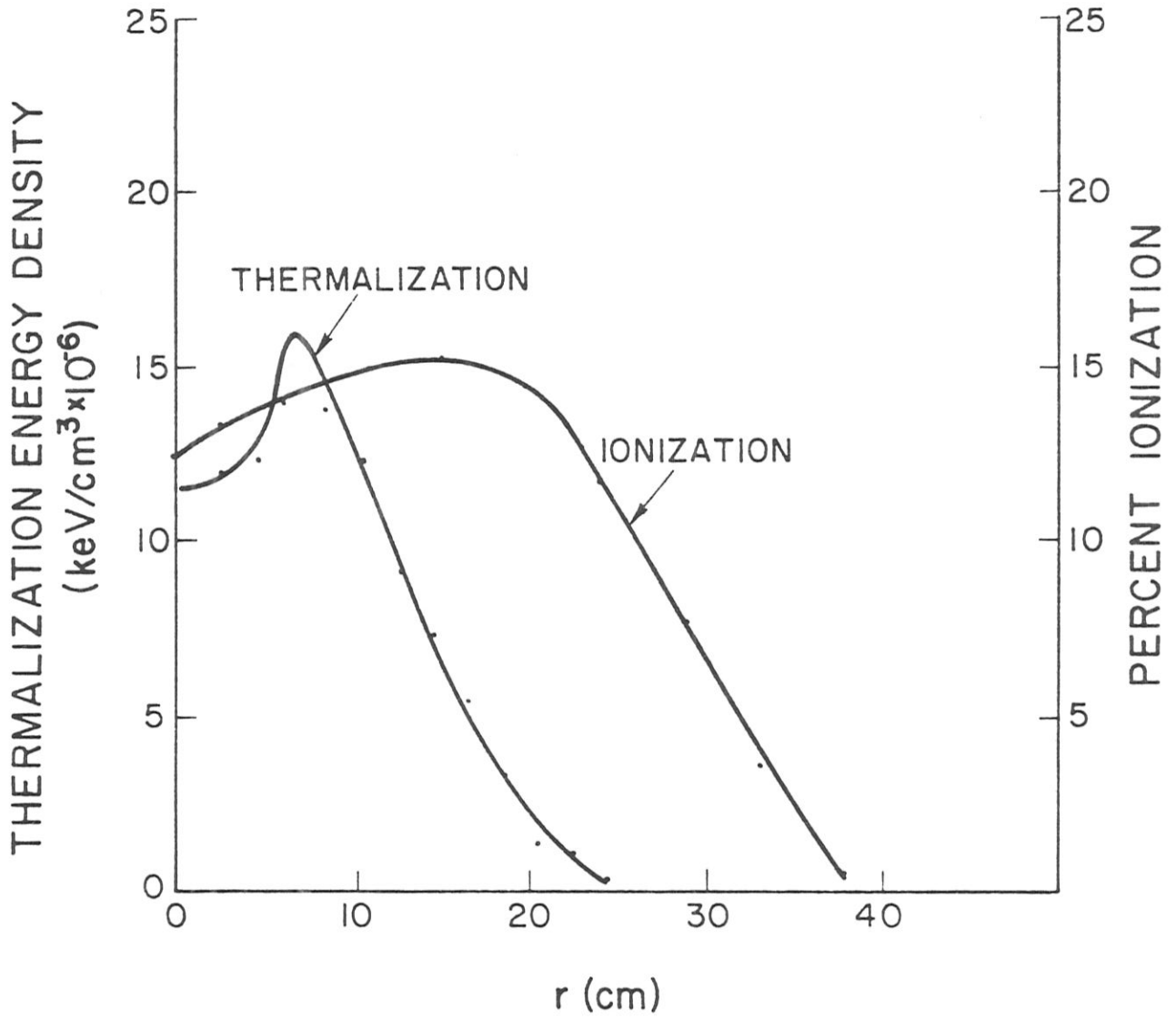
THERMALIZATION ENERGY DENSITY
(keV/cm³x10⁻⁶)
PERCENT IONIZATION
THERMALIZATION
IONIZATION
r (cm)
0
5
10
15
20
25
0
10
20
30
40

Figure 5b

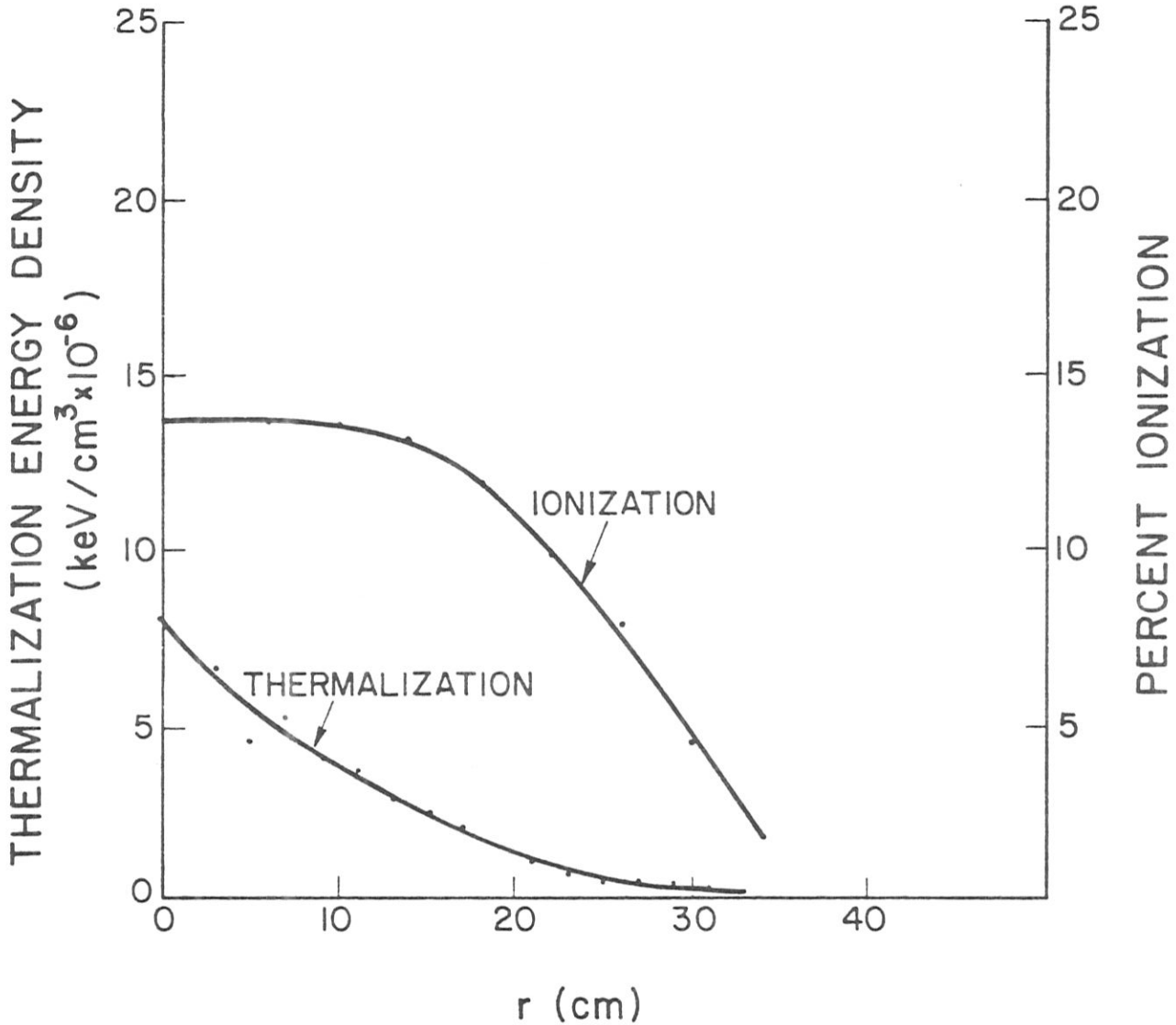
THERMALIZATION ENERGY DENSITY
(keV/cm³x10⁻⁶)
PERCENT IONIZATION
IONIZATION
THERMALIZATION
r (cm)
0
5
10
15
20
25
0
10
20
30
40

Figure 5c

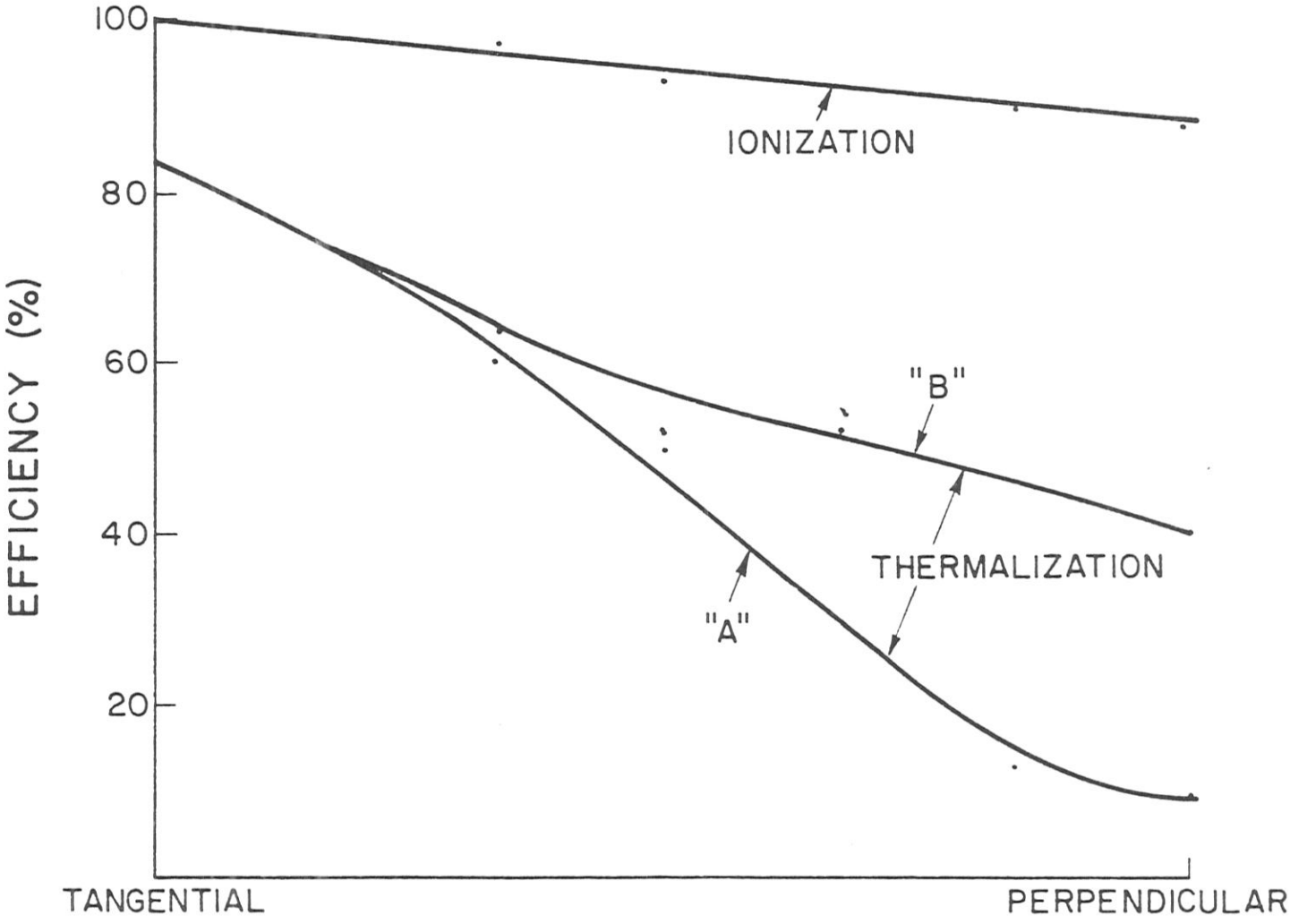
100
80
60
40
20
EFFICIENCY (%)
IONIZATION
"B"
THERMALIZATION
"A"
TANGENTIAL
PERPENDICULAR
INJECTION ANGLE

Figure 6

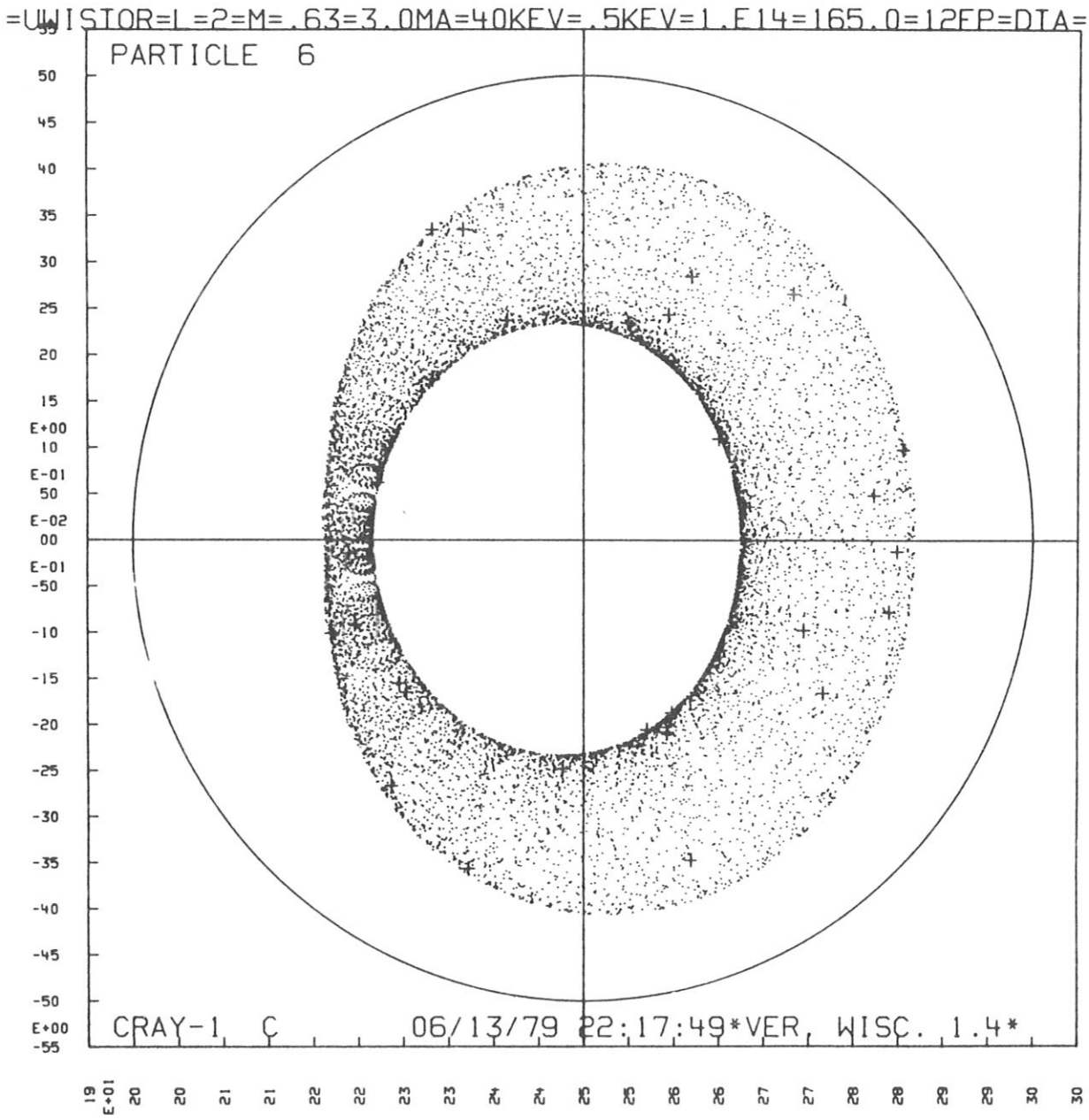
=UWISTOR=L=2=M=.63=3.0MA=40KEV=.5KEV=1.E14=165.0=12FP=DIA=
PARTICLE 6
CRAY-1 C
06/13/79 22:17:49*VER, WISC. 1.4*

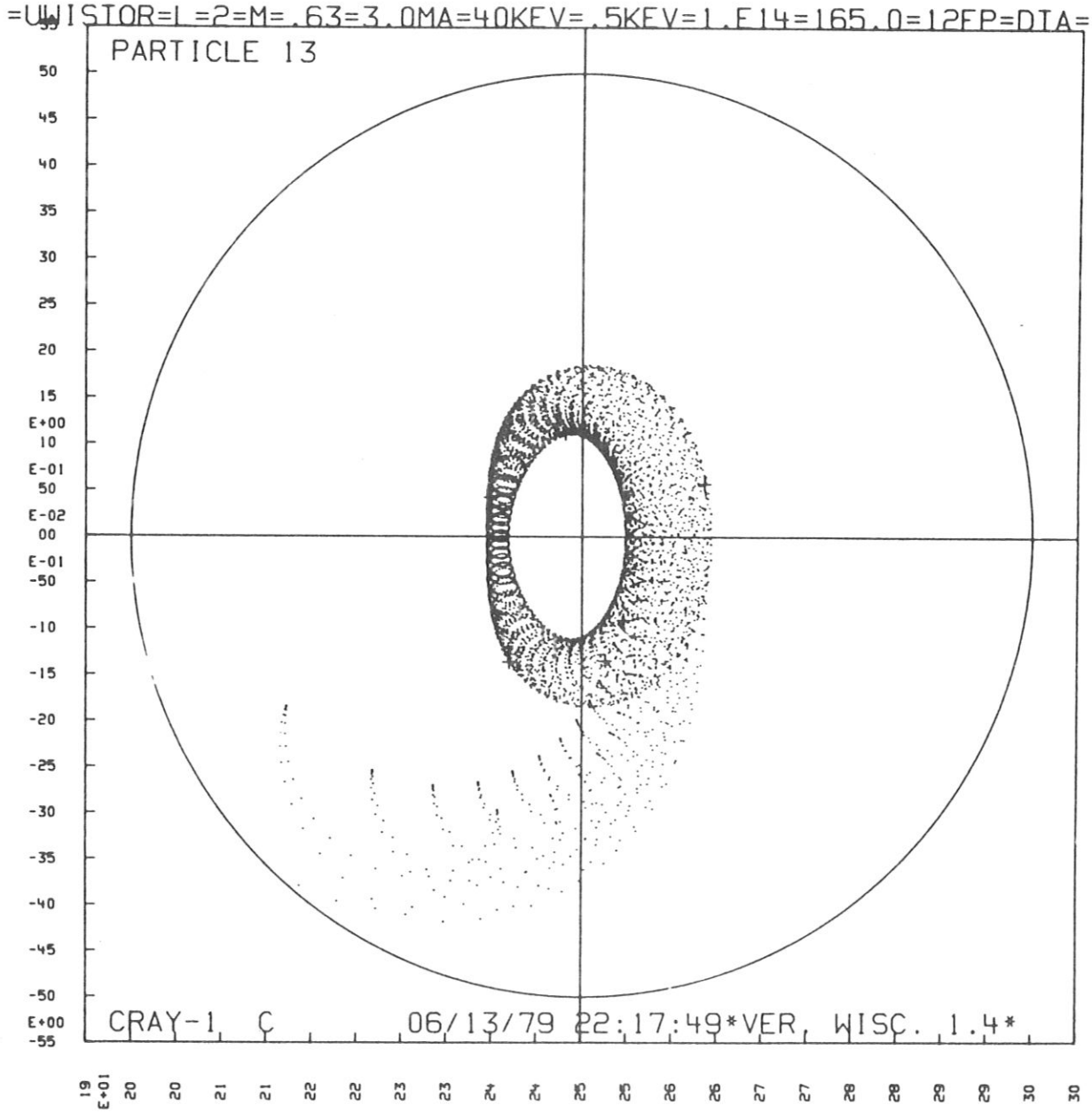
=UWISIOR=L=2=M=.63=3.0MA=40KEV=.5KEV=1.E14=165.0=12EP=DIA=
PARTICLE 13
CRAY-1 C
06/13/79 22:17:49*VER. WISC. 1.4*

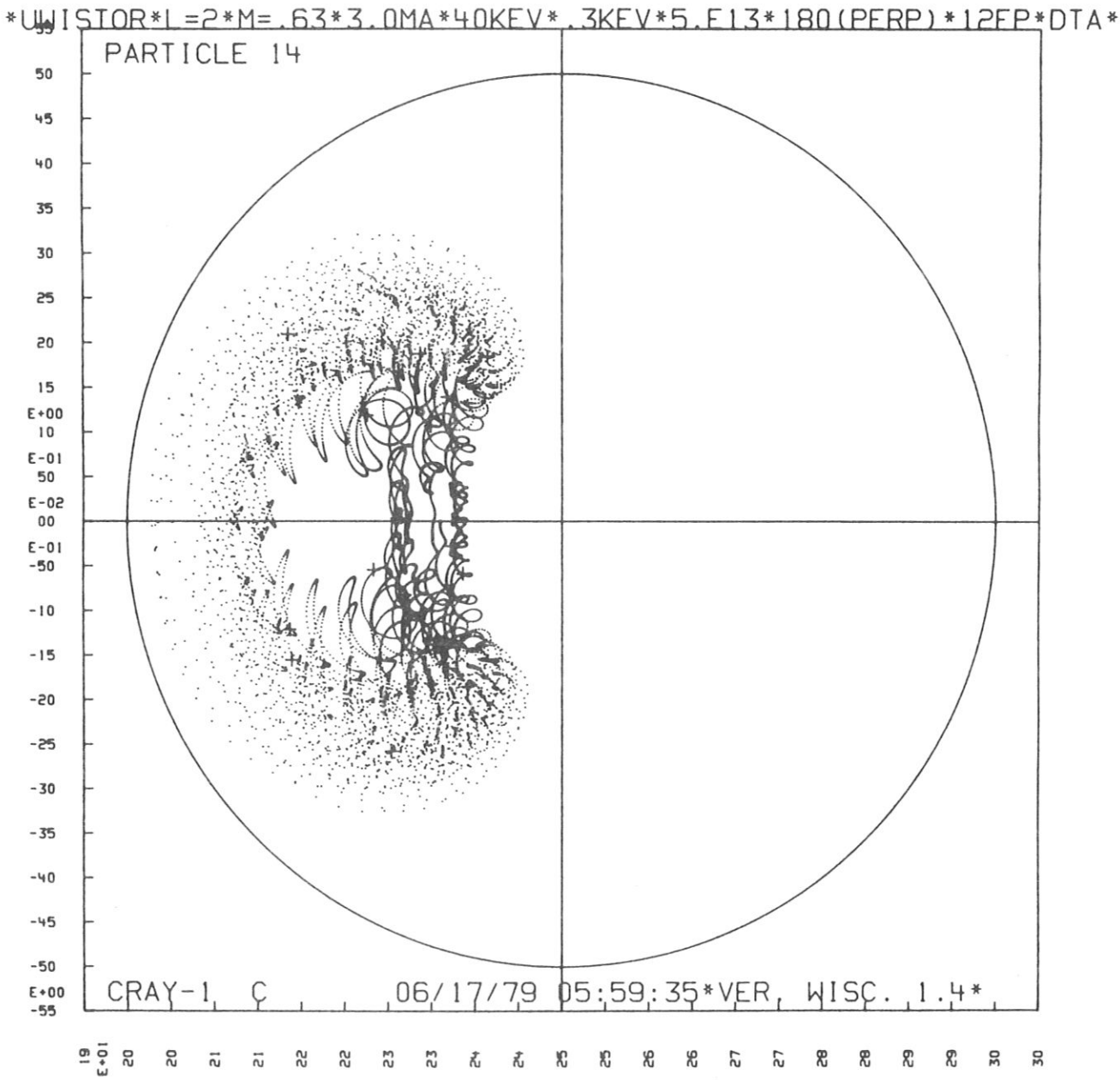
*UWISTOR*L=2*M=.63*3.0MA*40KEV*.3KEV*5.E13*180(PERP)*12FP*DTA*
PARTICLE 14
CRAY-1 C 06/17/79 05:59:35*VER. WISC. 1.4*